Improving Pheromone Communication for UAV Swarm Mobility Management

Daniel H. Stolfi[1][0000−0002−1138−8130], Matthias R. Brust[1][0000−0001−8155−0626], Grégoire Danoy[1,2][0000−0001−9419−4210], and Pascal Bouvry[1,2][0000−0001−9338−2834]

[1] Interdisciplinary Centre for Security, Reliability and Trust (SnT), University of Luxembourg, Esch-Sur-Alzette, Luxembourg
{daniel.stolfi,matthias.brust}@uni.lu
[2] FSTM/DCS, University of Luxembourg, Esch-Sur-Alzette, Luxembourg
{gregoire.danoy,pascal.bouvry}@uni.lu

Abstract. In this article we address the optimisation of pheromone communication used for the mobility management of a swarm of Unmanned Aerial Vehicles (UAVs) for surveillance applications. A genetic algorithm is proposed to optimise the exchange of pheromone maps used in the CACOC (Chaotic Ant Colony Optimisation for Coverage) mobility model which improves the vehicles' routes in order to achieve unpredictable trajectories as well as maximise area coverage. Experiments are conducted using realistic simulations, which additionally permit to assess the impact of packet loss ratios on the performance of the surveillance system, in terms of reliability and area coverage.

Keywords: unmanned aerial vehicle · pheromones · evolutionary algorithm · surveillance system · swarm robotics · mobility model.

1 Introduction

Unmanned Aerial Vehicles (UAVs) initially developed for military applications are nowadays paving their way into multiple civilian domains [10]. These include cargo delivery, road traffic surveillance, fire fighting, environmental monitoring, architecture surveillance, and farming. Considering surveillance applications [19], UAVs allow to provide a mobile and controllable bird's-eye view for a fraction of the cost existing solutions (e.g. helicopters). However, UAVs are typically small to medium size battery powered devices which therefore feature limited flight time and payload capacity. One promising approach to overcome those limitations is to use multiple autonomous UAVs simultaneously, also referred to as a swarm, where collaborations with other types of vehicles [18] are possible.

Unpredictability of vehicle trajectories [5] in surveillance scenarios is a desired characteristic to prevent the use of possible detection strategies, especially in military applications where an attacker is present. Some mobility models, like CROMM (Chaotic Rössler Mobility Model) [13], use chaotic trajectories to avoid route prediction but UAVs tend to visit the same locations frequently. CACOC

(Chaotic Ant Colony Optimisation for Coverage) [13] is another chaos based mobility model conceived to address that issue by using virtual pheromones, shared between UAVs to improve area coverage. These pheromones must be efficiently exchanged between UAVs to ensure a good global performance of the swarm. However, communications in such highly dynamic *ad hoc* networks are very challenging [8].

This article proposes to evaluate and optimise the communications between autonomous UAVs as members of a swarm performing surveillance tasks. More precisely, the parameters of CACOC+ (a parameterised version of CACOC) are optimised using a genetic algorithm in order to maximise area coverage, even when communications are restricted in packet size, and UAVs have to base their mobility decisions on their own local data, e.g. their virtual pheromone map. Experiments using realistic simulations permit to consider limited communication range, transmissions consuming energy, and radio packets that might be lost before reaching destination due to interferences.

The remainder of this paper is organised as follows. In the next section, we review the state of the art related to our proposal. In Section 3 our approach is presented. The optimisation algorithm is described in Section 4. Our case studies and experimental results are presented and analysed in Section 5. Finally, Section 6 brings discussion and future work.

2 Related Work

UAV communications has been addressed by several authors. In [1] a concept-level proposal and literature review for the use of cellular networks as the communication infrastructure for UAV swarms is presented. The authors highlight the practically unlimited range of communications using cellular data coverage (3G in the United States) and the reliability of its base stations. This proposal is tested in the real world using custom built quadcopters and the MAVLink communication protocol [3]. In [11] the authors address the problem of UAV swarm formation in areas covered by 3G/4G mobile networks and present an algorithm for multi-robot coordination which is also bandwidth-efficient. The proposed protocol for UAV coordination uses the group-cast and group management facilities of the authors' mobile communication middleware. Several test were done in a swarm of ten simulated UAVs.

In [4] a study about communication performance between UAVs in the 2.4 GHz band is presented. It takes into account how existing interferences and packet loss ratio affect a stable communication link. Their findings include that the degree of vibration generated by propellers interferes with the link signal, although the larger interferences come from the remote controllers, since they work in the same frequency band. Delay in the wireless network and its stability are analysed in [21]. A swarm of three cellular-connected UAVs, positioned in a triangle formation, is proposed to be optimised. The maximum allowable delay required to prevent the instability of the swarm is also analysed. Path planning for multiple robots for persistent surveillance with connectivity constraints is

studied in [15]. Greedy and cooperative strategies are proposed for the robots to reach all sensing locations, being the performance of the former higher when the number of robots or the communication range is large enough.

In this article we focus on the optimisation of the communications between UAVs by controlling the amount of data shared by drones during their interactions. The use of *ad hoc* communications allows to work in a private network with an increment in the security of the radio links. Although reliable communications are assumed, we investigate the consequences of packet loss. To the best of our knowledge, this study involving the optimisation of the parameters of CACOC+, to deal with communication constraints and pheromone maps, has not been done before. In the following section we describe CACOC+, followed by the bio-inspired algorithm proposed for optimising its parameters.

3 Pheromone Based Swarm Mobility

In a previous article [16] the optimisation of the CACOC mobility model to maximise area coverage was proposed. CACOC is a mobility model for UAV swarms that uses chaotic dynamics and pheromone methods for improving area coverage using unpredictable trajectories. When using CACOC, UAVs leave pheromones as they move in the environment to indicate recently covered areas. Pheromones have a repulsive effect and thus, aim to better spread UAVs in the area avoiding visiting the same spots too frequently. As pheromone trails evaporate, a UAV will eventually visit again the same region of the map.

The diagram of CACOC is shown in Fig. 1. The next moving direction is calculated using chaotic dynamics when there are no pheromones in the UAV's neighbourhood. Values from the first return map (ρ) from a chaotic attractor, obtained by solving a Rössler ordinary differential equation system [14], are used to replace the random part of the mobility model, as proposed in [13]. On the other hand, when virtual pheromones are detected, they work as repellers, stochastically modifying the UAV's next moving direction. The amount of pheromones detected in each scanned direction is used to calculate the probabilities $P_L = \frac{phe\_total - phe\_left}{2 \times phe\_total}$, $P_R = \frac{phe\_total - phe\_right}{2 \times phe\_total}$, for the next move.

In [16], three parameters for CACOC were proposed to adapt this model to different scenarios and improve area coverage (it will be referred to as CACOC+ hereafter). These parameters are depicted in Fig. 2, and are described as: the optimised amount of pheromones left by each vehicle (τ_a), the pheromone radius (τ_r) and maximum detection distance (τ_d). The pheromone decay rate used is the same value as in CACOC, i.e. one unit per second.

3.1 Pheromone Communication

In previous works, CACOC and CACOC+ assumed perfect communications, where vehicles were always in their respective communication range, and there was no packet loss. This article considers a more realistic scenario featuring limited communication ranges and interferences by using the well-known ARGoS

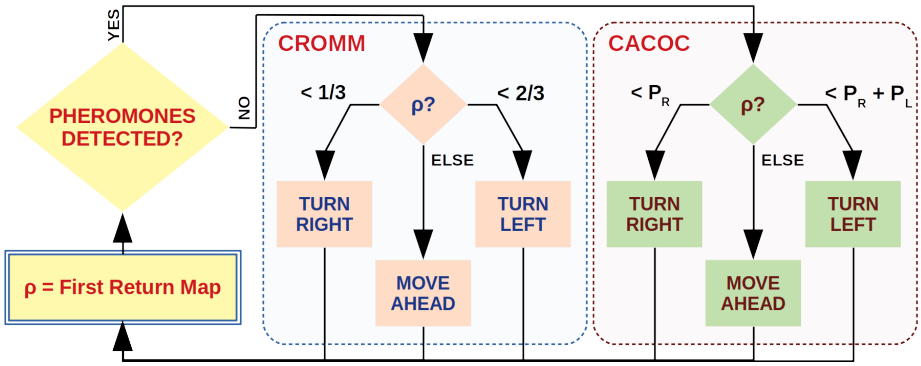

Fig. 1. Diagram of the CACOC (and CACOC+) mobility models.

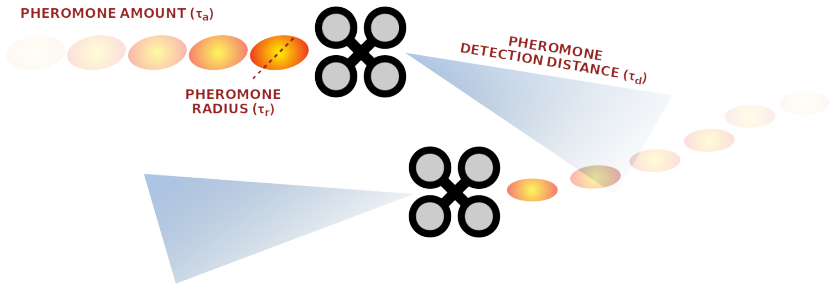

Fig. 2. Three parameters proposed for CACOC+.

simulator [12] and its communication model between robots. Additionally, in this study we address the validation of CACOC+ in a different simulator as it was previously tested only in the HUNTED Sim [17].

As part of a swarm of autonomous vehicles, each member has to take local decisions to achieve a common global goal, e.g. maximising area coverage. In CACOC+ each vehicle has its own local pheromone map composed by its own pheromone trails and portions of pheromone maps received from the other vehicles in the scenario (figures 3(b) and 3(c)). They are shared by using *ad hoc* communications which are subject to disruptions and interferences. The complete pheromone map is represented in Fig. 3(a).

Moreover, larger data packets imply more energy consumption and a higher probability of data loss. Consequently, we propose the optimisation of the CACOC+ parameters where UAVs share different amount of data, and an analysis of how it affects the system performance when each swarm member only knows partially the pheromone map. Therefore, our problem representation is the vector $\boldsymbol{x} = \{\tau_{a_1}, \tau_{r_1}, \tau_{d_1}, \ldots, \tau_{a_N}, \tau_{r_N}, \tau_{d_N}\}$ where N is the number of UAVs in the swarm. Thus, vector $\boldsymbol{x}$ defines the configuration of the surveillance system which comprises the parameters of each UAV in the swarm represented by integer val-

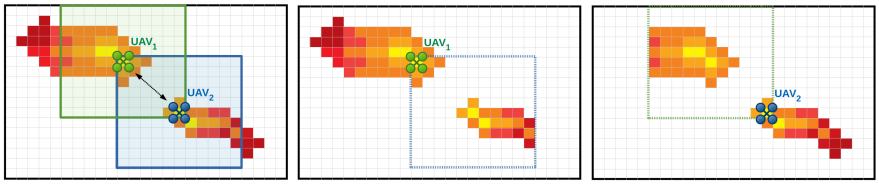

(a) Full pheromone map (b) UAV$_1$'s known map (c) UAV$_2$'s known map

Fig. 3. Pheromone map shared between UAVs according to their communication range. Each UAV knows its own map and the map portions received from the others (dashed squares in (b) and (c)).

ues. Note that the amount of shared pheromones is not included in the problem representation since it is part of the characteristics of each case study.

3.2 Collision Avoidance

The implemented collision avoidance algorithm relies on repelling forces between UAVs. Given $u \in UAVs$, the distances between u and the rest of vehicles in $UAVs$ are calculated. Those UAVs closer than a minimum distance δ_{min} (a fixed parameter, e.g. 6 metres) modify the vector $\boldsymbol{r_u}$, which will contain the resultant repelling force for u, to be used to modify its trajectory.

We have implemented this straightforward algorithm as UAVs following their mobility model decisions will eventually divert to no colliding trajectories avoiding any possible deadlock. As a consequence of the implemented algorithm, which requires to know the position of the other UAVs in the neighbourhood, communications between vehicles also include the coordinates of the transmitting UAV.

4 Optimisation Algorithm

We have designed a Genetic Algorithm (GA) which uses operators for continuous optimisation, in order find the parameterisation of CACOC+ which maximises the area coverage for different pheromone block sizes shared between UAVs. The proposed GA is based on an Evolutionary Algorithm (EA) [6, 9] which is an efficient method for solving combinatorial optimisation problems. EAs simulate processes present in evolution such as natural selection, gene recombination after reproduction, gene mutation, and the dominance of the fittest individuals over the weaker ones. This is a generational GA where an offspring of λ individuals is obtained from the population μ, so that the auxiliary population Q contains the same number of individuals as the population Pop. The number of individuals was set to 16 since their evaluations require expensive simulations.

Algorithm 1 shows the pseudocode of the GA. After initializing t and $Q(0)$, $Pop(0)$ is generated by using the *Initialization* function. Then, the main loop is executed while the *TerminationCondition* is not fulfilled (in our case we stop after 1,000 evaluations). Into the main loop, the *Selection* operator is applied

Algorithm 1 Pseudocode of the Genetic Algorithm (GA).

```
procedure GA(N_i, P_c, P_m)
    t ← ∅
    Q(0) ← ∅                                   ▷ Q=auxiliary population
    Pop(0) ← Initialization(N_i)               ▷ Pop=population
    while not TerminationCondition() do
        Q(t) ← Selection(Pop(t))
        Q(t) ← Crossover(Q(t), P_c)
        Q(t) ← Mutation(Q(t), P_m)
        Evaluation(Q(t))
        Pop(t + 1) ← Replacement(Q(t), Pop(t))
        t ← t + 1
```

to populate $Q(t)$ using Binary Tournament [7]. Next, the *Crossover* operator is applied and after that, the *Mutation* operator slightly modifies the new offspring. Finally, after the *Evaluation* of $Q(t)$, the new population $Pop(t+1)$ is obtained by applying the *Replacement* operator. It consists in selecting the best individual in $Q(t)$ to replace the worst one in $Pop(t)$ if it is best valued [2]. This contributes to avoid population stagnation and preserves its diversity.

4.1 Crossover Operator

The crossover operator implements the one-point crossover [9] using vehicle configuration blocks. Two individuals $\boldsymbol{x}$ and $\boldsymbol{y}$ are taken from the population Q and the recombination operator is applied to them if a generated random number is less than the crossover probability $P_c = 0.9$. The crossing point is then calculated using a uniformly distributed, random integer value cp. The crossover is made at UAV level: as there are three parameters per UAV, possible values of cp are 3, 6, 9, etc. The UAVs' configurations in $\boldsymbol{x}$ and $\boldsymbol{y}$ after the cp-th position are swapped and added to the destination population $Q\prime$. This process is repeated for the rest of the individuals in Q (taken in groups of two) to complete the new population $Q\prime$, to be subject to mutation.

4.2 Mutation Operator

The mutation operator (Algorithm 2) is based on the one proposed in [2], and adapted to our problem characteristics. First, each position of the individual $\boldsymbol{x}$ in Q is subject to mutation according to the mutation probability $P_m = \frac{1}{L}$, where L is the length of the solution vector. If a component of $\boldsymbol{x}$ is selected for mutation, a new M value is randomly calculated according to a uniform probability distribution. Then, the value of Δ is obtained taking into account the bounds of the parameter associated to each component of $\boldsymbol{x}$, and k (Equation 1). The value of k begins in 1 and exponentially decreases during the execution of the algorithm to increase the exploration in the early stages and focus on the exploitation of the solutions found, in the last generations of the GA.

Algorithm 2 Pseudocode of the Mutation Operator.

```
function MUTATION(Q, P_m, k)
    Q' ← ∅
    for {x} ∈ Q do
        x' ← x
        for i ← 1, L do                                   ▷ L = length(x)
            if rnd() < P_m then                           ▷ mutation probability
                M ← randInt(1, 10)
                if rnd() < 0.5 then                       ▷ increment/decrement
                    x'[i] ← min(x[i] + Δ(i, M, k), UpBd(x[i]))
                else
                    x'[i] ← max(x[i] − Δ(i, M, k), LowBd(x[i]))
        Q' ← Q' ∪ {x'}
    return Q'
```

$$\Delta(i, M, k) = k \times \frac{UpBd(x[i]) - LowBd(x[i])}{M} \tag{1}$$

The current value of the parameter in the solution vector is either increased or decreased (equally probable) taking into account the parameters' bounds, and finally, the new individual $\boldsymbol{x\prime}$ is added to the new population $Q\prime$.

4.3 Fitness Function

Our objective is maximising the covered area to improve the surveillance performed by the UAV swarm under different communication restrictions. Therefore, the evaluation of each system configuration is achieved taking into account the percentage of area visited during the simulation time (600 seconds). Each scenario is mapped as a lattice of 100x100 cells for evaluation purpose. We assumed that a UAV explores an area of 3x3 cells at each simulation tick (note that they are still moving in the continuous coordinated space provided by ARGoS). Consequently, the fitness value of a given configuration is calculated as shown in Equation 2. As we are maximising the explored area, the higher the value of $F(\boldsymbol{x})$, the better.

$$F(\boldsymbol{x}) = \frac{\#\ of\ explored\ cells}{\#\ of\ cells\ in\ the\ scenario} \tag{2}$$

5 Experiments

In this section we describe our case studies, perform the optimisation of CACOC+, compare its performance against CROMM and CACOC, and analyse the effects of packet loss. Our experiments were conducted in parallel on computing nodes equipped with Intel Xeon Gold 6132 @ 2.6 GHz and 128 GB of RAM. The total optimisation time was equivalent to 12 days.

5.1 Case Studies

We propose three case studies consisting in four scenarios each, where different amount of pheromones are shared. Swarms of two, four and six UAVs are analysed in each case study respectively, which begin their surveillance tasks in the centre of the map. The four possible scenarios are: i) CACOC+ where the entire pheromone map is shared between UAVs in communication range, ii) CACOC+.10 where a square of 21x21 cells is shared, iii) CACOC+.05 where a square of 11x11 cells is shared, and iv) CACOC+.00 where no pheromone map is shared between UAVs.

The communication range is set to 10 metres where the collision avoidance algorithm also takes place. Consequently, the communication packet also includes the UAV's identifier (8 bits) and its 2-D coordinates (2 x 32 bits) as every UAVs is assumed to fly at the same altitude. All in all, packet length is 10,009 bytes in CACOC+, 450 bytes in CACOC+.10, 130 bytes in CACOC+.05, and 9 bytes in CACOC+.00. Note that this is actually the payload of the communication packet as we are not considering protocol specific data in our study. The communication layer used was "range and bearing" as provided by ARGoS.

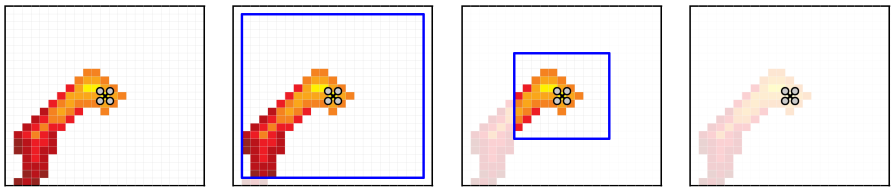

(a) CACOC+ (b) CACOC+.10 (c) CACOC+.05 (d) CACOC+.00

Fig. 4. Pheromone transmission scenarios. In CACOC+ each UAV shares all its pheromone map (10,000 cells). UAVs share 441 cells in CACOC+.10, 121 cells in CACOC+.05, and none in CACOC+.00.

Fig. 4 shows an example of the pheromone map shared by a UAV via *ad hoc* wireless communications corresponding to each scenario analysed in our approach. It is worth mentioning that each UAV has access to its own pheromone map at any time. What a UAV receives is the portion of the global pheromone map transmitted (known) by the other (neighbouring) UAVs. We assumed that at the flying altitude there are no obstacles in the scenario.

5.2 CACOC+ Optimisation

We have performed 30 independent runs of the proposed GA on each case study and scenario, i.e. 360 runs in total. GA was configured to stop after 1,000 evaluations, a population of 16 individuals ($\lambda = \mu = 16$), 0.9 as crossover probability (P_c), and $\frac{1}{L}$ as mutation probability (P_m). The results obtained during the optimisation process are shown in Table 1.

Table 1. Optimisation results: fitness values (average, standard deviation, and maximum) of each optimisation run for each case study and scenario.

Case Study	Scenario	Fitness			Friedman Rank	Wilcoxon p-value
		Avg.	SD.	Max.		
2 UAVs	CACOC+	0.524	0.005	0.538	2.50	0.365
	CACOC+.10	0.523	0.006	0.535	2.10	0.325
	CACOC+.05	0.525	0.006	0.535	2.68	0.802
	CACOC+.00	**0.526**	0.007	**0.539**	**2.72**	—
4 UAVs	CACOC+	0.769	0.006	0.780	2.28	0.087
	CACOC+.10	0.771	0.007	**0.788**	2.70	0.640
	CACOC+.05	0.769	0.005	0.782	2.22	0.120
	CACOC+.00	**0.772**	0.006	0.786	**2.80**	—
6 UAVs	CACOC+	0.885	0.005	0.895	2.48	0.246
	CACOC+.10	**0.887**	0.004	**0.897**	**2.70**	—
	CACOC+.05	0.885	0.004	0.893	2.52	0.133
	CACOC+.00	0.884	0.006	0.896	2.30	0.058

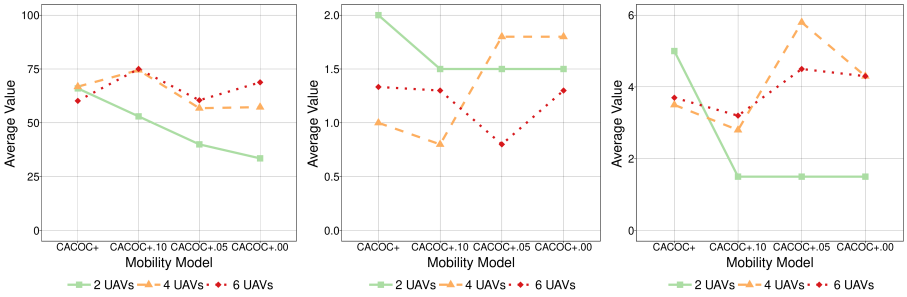

(a) Phero amount (τ_a) (b) Phero radius (τ_r) (c) Detection distance (τ_d)

Fig. 5. Average values of the CACOC+'s optimised parameters for each UAV.

It can be seen that CACOC+ achieves very similar results for all the scenarios of each case study. Best average fitness values of CACOC+ for 2 UAVs are 0.526, 0.772 for 4 UAVs, and 0.887 for 6 UAVs. Statistical tests (Friedman Rank and Wilcoxon p-value) show that the differences between the results of each case study are not statistically significant (p-value always greater than 0.01). This means that CACOC+ has compensated the lack of information about the global pheromone map by adapting their operational parameters to keep competitive fitness values, as shown in Fig. 5. Two UAVs show a clear parameter decreasing pattern when less data are shared, although the others case studies do not present such a pattern. We believe that it is due to the fact that there are more UAVs in the scenarios and the number of iterations (including collision avoidance) are higher as well as the complexity of the problem.

5.3 Experimental Results

The next experiment consisted in comparing the CACOC+ results against CACOC and CROMM. Table 2 shows the area coverage values of those mobility models. It can be seen that the values achieved by CACOC+ are consistent with the fitness values previously reported. UAVs using CACOC cover less area than CACOC+ as expected. When the UAVs controlled by CACOC were subject to the same communication restrictions as CACOC+, their coverage values showed bigger variability, being notably affected by the amount of pheromones shared between them, especially when there are more pheromones in the scenario (more UAVs). Note that each UAV still has access to its own pheromone map even if there is no communication with its counterparts.

The lowest CROMM coverage values confirm the need of virtual pheromones as a complement of chaotic mobility to improve the area coverage of the surveillance system. All in all, CACOC+ covered up to 53.9% of the surveillance area when using 2 UAVs, up to 78.8% when using 4 UAVs, and up to 89.7% when using 6 UAVs. That represents a maximum increment of around 7% with respect to CACOC and of around 41% with respect to CROMM. When there are communication restrictions, CACOC+ shown increments up to 15% in area coverage. Note that unpredictable chaotic trajectories perform unexpected turns and usually visit the same spot (despite pheromones). This is a desired feature in a surveillance system which, in turn, reduces the total area explored by UAVs compared with a highly predictable lawnmower model.

Table 2. Area coverage achieved by each scenario of CACOC+. CROMM and CACOC with the same communication restrictions are also included for comparison.

Case Study	2 UAV	4 UAV	6 UAV
CROMM	13.3%	43.5%	52.2%
CACOC	46.5%	71.0%	85.8%
CACOC.10	46.5%	68.7%	85.8%
CACOC.05	46.5%	71.6%	84.2%
CACOC.00	38.8%	70.2%	80.0%
CACOC+	53.8%	78.0%	89.5%
CACOC+.10	53.5%	**78.8%**	**89.7%**
CACOC+.05	53.5%	78.2%	89.3%
CACOC+.00	**53.9%**	78.6%	89.6%

5.4 Interferences and Packet Loss

The last study comprises an analysis about the resilience of CACOC+ when it is subject to interferences, e.g. packet loss. Fig. 6 shows the area coverage achieved by CACOC+ subject to different packet loss probabilities. Since the collision

avoidance algorithm also uses radio communications to detect and avoid other UAVs, the vehicle trajectories were also affected by these new late detections as seen in CACOC+.00. Moreover, we were unable to complete our tests up to 100% packet loss for 4 and 6 UAVs since some vehicles were closer than the safety threshold (2 metres) and the simulation was stopped. The amount of area covered decreased when the communication link failed, as expected. However, in most of the analysed scenarios, before reaching very low coverage values, the rest of the system features were degraded, e.g. the collision avoidance algorithm, especially when the number of UAVs was higher and the collisions were more probable. It can be seen a small increment in the area coverage for some case studies at higher packet loss probabilities. Even if the maximum coverage (at zero packet loss) is never reached, this counter-intuitive behaviour has to be further analysed in a future work.

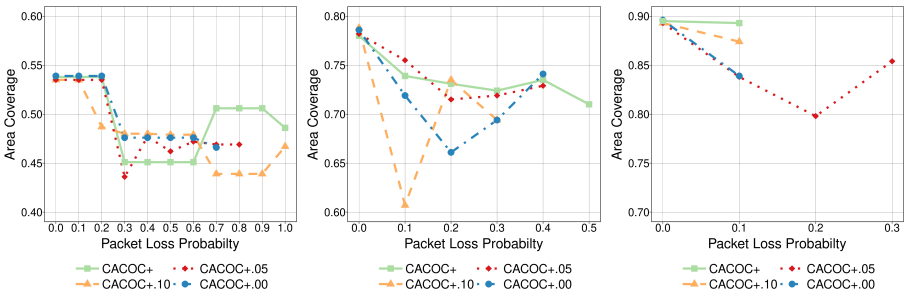

(a) 2 UAVs (b) 4 UAVs (c) 6 UAVs

Fig. 6. Area coverage achieved using CACOC+ vs. packet loss probability.

6 Conclusions and Future Work

In this article we have proposed a more realistic approach to a swarm of UAVs using the CACOC mobility model by modelling real communication links. We have optimised its parameterised version, CACOC+, initially proposed to improve area coverage, with the aim of keeping good performance values even when each UAV knows only its own local pheromone map. The well-known simulator ARGoS was used in our experimentation to implement the mobility models and the data transmission layer.

Our results show that CACOC+ still improves CACOC under these new conditions and that the versatility of the UAV parameterisation has compensated the reduced knowledge of the pheromone neighbourhood. Furthermore, the UAVs trajectories, now adapted to the new environmental conditions, keep obtaining good coverage values until the defective communications affect other aspects of the system, such as the collision avoidance algorithm.

As larger data packets increase the probability of transmission errors, CA-COC+ showed to be more resilient to communications failures as the amount of transmitted data can easily be reduced from 10,009 to 9 bytes (99.9% shorter) without experiencing a reduction of the area explored by UAVs. The energy consumed by vehicles was not analysed but it is assumed to be lower as their onboard radio has a reduced duty cycle.

As a matter of future work we would like to test our approach on larger scenarios, including more UAVs, and improve the system precision by using a specific parameter for each UAV, to define the portion of its pheromone map to be shared with the others. The analysis of the influence of each parameters on the results is another interesting future work. An alternative collision avoidance algorithm is to be tested using, for example, a different approach based on on-board sensors. Finally, we intend to validate our trajectories using real drones and also extend our analysis taking into account power consumption.

7 Acknowledgments

This work relates to Department of Navy award N62909-18-1-2176 issued by the Office of Naval Research. The United States Government has a royalty-free license throughout the world in all copyrightable material contained herein. This work is partially funded by the joint research programme UL/SnT-ILNAS on Digital Trust for Smart-ICT. The experiments presented in this paper were carried out using the HPC facilities of the University of Luxembourg [20] – see https://hpc.uni.lu.

References

1. Campion, M., Ranganathan, P., Faruque, S.: UAV swarm communication and control architectures: A review. Journal of Unmanned Vehicle Systems **7**(2), 93–106 (jun 2019). https://doi.org/10.1139/juvs-2018-0009
2. Chelouah, R., Siarry, P.: Continuous genetic algorithm designed for the global optimization of multimodal functions. Journal of Heuristics **6**(2), 191–213 (2000). https://doi.org/10.1023/A:1009626110229
3. Dronecode Project: MAVLink: Micro Air Vehicle Communication Protocol (2021), https://mavlink.io/en/
4. Fabra, F., Calafate, C.T., Cano, J.C., Manzoni, P.: On the impact of inter-UAV communications interference in the 2.4 GHz band. In: 2017 13th International Wireless Communications and Mobile Computing Conference (IWCMC). pp. 945–950. IEEE (jun 2017). https://doi.org/10.1109/IWCMC.2017.7986413
5. Galceran, E., Carreras, M.: A survey on coverage path planning for robotics. Robotics and Autonomous Systems **61**(12), 1258–1276 (dec 2013). https://doi.org/10.1016/j.robot.2013.09.004
6. Goldberg, D.E.: Genetic Algorithms in Search, Optimization and Machine Learning. Addison-Wesley Longman Publ. Co., Inc., Boston, MA, USA, 1st edn. (1989)
7. Goldberg, D.E., Deb, K.: A Comparative Analysis of Selection Schemes Used in Genetic Algorithms. Foundations of Genetic Algorithms **1**, 69–93 (1991). https://doi.org/10.1.1.101.9494

8. Gupta, L., Jain, R., Vaszkun, G.: Survey of Important Issues in UAV Communication Networks. IEEE Communications Surveys & Tutorials **18**(2), 1123–1152 (2016). https://doi.org/10.1109/COMST.2015.2495297
9. Holland, J.H.: Adaptation in Natural and Artificial Systems. The MIT Press (1992). https://doi.org/10.7551/mitpress/1090.001.0001
10. McNeal, G.S.: Drones and the Future of Aerial Surveillance. George Washington Law Review Arguendo **84**(2), 354–416 (2016)
11. Olivieri de Souza, B.J., Endler, M.: Coordinating movement within swarms of UAVs through mobile networks. In: 2015 IEEE International Conference on Pervasive Computing and Communication Workshops (PerCom Workshops). pp. 154–159. IEEE (mar 2015). https://doi.org/10.1109/PERCOMW.2015.7134011
12. Pinciroli, C., Trianni, V., O'Grady, R., Pini, G., Brutschy, A., Brambilla, M., Mathews, N., Ferrante, E., Di Caro, G., Ducatelle, F., Birattari, M., Gambardella, L.M., Dorigo, M.: ARGoS: a modular, parallel, multi-engine simulator for multi-robot systems. Swarm Intelligence **6**(4), 271–295 (dec 2012). https://doi.org/10.1007/s11721-012-0072-5
13. Rosalie, M., Danoy, G., Chaumette, S., Bouvry, P.: Chaos-enhanced mobility models for multilevel swarms of UAVs. Swarm and Evolutionary Computation **41**(November 2017), 36–48 (2018). https://doi.org/10.1016/j.swevo.2018.01.002
14. Rosalie, M., Letellier, C.: Systematic template extraction from chaotic attractors: II. Genus-one attractors with multiple unimodal folding mechanisms. Journal of Physics A: Mathematical and Theoretical **48**(23), 235101 (jun 2015). https://doi.org/10.1088/1751-8113/48/23/235101
15. Scherer, J., Rinner, B.: Multi-robot persistent surveillance with connectivity constraints. IEEE Access **8**, 15093–15109 (2020). https://doi.org/10.1109/ACCESS.2020.2967650
16. Stolfi, D.H., Brust, M.R., Danoy, G., Bouvry, P.: A Cooperative Coevolutionary Approach to Maximise Surveillance Coverage of UAV Swarms. In: 2020 IEEE 17th Annual Consumer Communications and Networking Conference, CCNC 2020. pp. 1–6. IEEE (jan 2020). https://doi.org/10.1109/CCNC46108.2020.9045643
17. Stolfi, D.H., Brust, M.R., Danoy, G., Bouvry, P.: Competitive evolution of a UAV swarm for improving intruder detection rates. In: 2020 IEEE International Parallel and Distributed Processing Symposium Workshops (IPDPSW). pp. 528–535. IEEE (May 2020). https://doi.org/10.1109/IPDPSW50202.2020.00094
18. Stolfi, D.H., Brust, M.R., Danoy, G., Bouvry, P.: Emerging Inter-Swarm Collaboration for Surveillance Using Pheromones and Evolutionary Techniques. Sensors **20**(9) (2020). https://doi.org/10.3390/s20092566
19. Stolfi, D.H., Brust, M.R., Danoy, G., Bouvry, P.: UAV-UGV-UMV Multi-Swarms for Cooperative Surveillance. Frontiers in Robotics and AI **8** (feb 2021). https://doi.org/10.3389/frobt.2021.616950
20. Varrette, S., Bouvry, P., Cartiaux, H., Georgatos, F.: Management of an academic HPC cluster: The UL experience. In: 2014 International Conference on High Performance Computing & Simulation (HPCS). pp. 959–967. IEEE, Bologna, Italy (jul 2014). https://doi.org/10.1109/HPCSim.2014.6903792
21. Zeng, T., Mozaffari, M., Semiari, O., Saad, W., Bennis, M., Debbah, M.: Wireless Communications and Control for Swarms of Cellular-Connected UAVs. In: 2018 52nd Asilomar Conference on Signals, Systems, and Computers. pp. 719–723. IEEE (oct 2018). https://doi.org/10.1109/ACSSC.2018.8645472